Available online at www.sciencedirect.com
SCIENCE DIRECT®
Nuclear Instruments and Methods in Physics Research B 244 (2006) 56–59
NIM B
Beam Interactions with Materials & Atoms
www.elsevier.com/locate/nimb

Studies on the formation of Si nanocrystals in SiO_2 by Ge ion implantation

P.K. Giri [a,*], R. Kesavamoorthy [b], B.K. Panigrahi [b], K.G.M. Nair [b]

[a] Department of Physics, Indian Institute of Technology Guwahati, Guwahati 781 039, Assam, India
[b] Materials Science Division, Indira Gandhi Center for Atomic Research, Kalpakkam 603 102, India

Available online 20 December 2005

Abstract

Ge ions are implanted on thermally grown SiO_2 layer at various doses and post-annealed in inert gas ambient. X-ray diffraction and Raman scattering studies on implanted samples reveal that Ge nanocrystals of sizes 4–13 nm are formed embedded in SiO_2 for Ge^+ ion fluence in the range 3×10^{16}–2×10^{17} cm^{-2}. At high dose ($\geqslant 1\times10^{17}$ cm^{-2}), in addition to Ge NCs, Si NCs are formed at the interface between Si and SiO_2 layer as a result of ion impact. Optical Raman spectra show distinct peak at $\sim$503 cm^{-1} corresponding to the Si NCs. Average size of the Si NCs are smaller than the average size of the Ge NCs.

PACS: 78.47.+p; 78.67.Bf; 61.46.+w; 78.55.−m

Keywords: Nanocrystals; Ion implantation; Raman scattering; XRD

1. Introduction

Over the last decade, there has been growing interest in synthesizing semiconductor nanocrystals (NCs) in SiO_2 because of their interesting optical [1] and electronic properties [2]. Several methods have been used to fabricate such structures [3,4]. Among these, ion beam synthesis has received considerable interest because of its ease and simplicity in growing NCs of varying size. Both Si [5] and Ge [6] NCs have been grown by implanting either Si^+ or Ge^+ ions into thermally grown SiO_2 films and subsequent annealing at temperatures of 800 °C or higher in inert gas environment. Due to their compatibility with microelectronics, both these group IV materials in nanocrystalline phase offer variety of applications in optoelectronic [7] and electronic memory [8] devices. However, growth of two different species of NCs by one-step ion implantation has not been reported. In this work, we show that Si NCs are formed at the SiO_2/Si interface due to Ge ion implantation at high doses, in addition to the formation of Ge NCs in the SiO_2 layer.

2. Experimental details

Before implantation, SiO_2 films were grown by wet oxidation of Si(100) wafer at 1000 °C for 4 h. Spectroscopic ellipsometry measurement shows an oxide thickness of $\sim$250 nm on the Si substrate. 300 keV Ge^+ ions were implanted at room temperature on the SiO_2 layer with doses 3×10^{16} (Ge1), 1×10^{17} (Ge2) and 2×10^{17} (Ge3) ions/cm^2 to grow nanocrystals of different sizes. SRIM calculation, a Monte Carlo code, shows that implanted Ge ions have a mean range of $\sim$206 nm with a straggling of $\sim$62 nm. SRIM calculation also shows that some of the Ge ions reach a depth of $\sim$350 nm below the top surface. We have studied the formation of embedded Ge and Si NCs after annealing the samples at 800 °C and 950 °C in argon gas atmosphere for several hours. We characterize these samples by X-ray diffraction (XRD) and Raman spectroscopy to identify the Ge and Si NCs. Raman spectra were recorded in the backscattering

* Corresponding author. Fax: +91 361 2690762.
E-mail address: giri@iitg.ernet.in (P.K. Giri).

0168-583X/$ - see front matter © 2005 Elsevier B.V. All rights reserved.
doi:10.1016/j.nimb.2005.11.017

geometry using vertically polarized 488 nm Ar^+ laser. XRD spectra were recorded using a powder diffractometer system in grazing incidence mode.

3. Results and discussion

Fig. 1 shows a set of grazing incidence XRD spectra on Ge2 and Ge3. Curves 1, 2 and 4 were obtained with grazing angle of 2° and curve 3 was obtained with an angle of 3°. Curve 1 is for Ge2 sample post-annealed at 800 °C, curves 2 and 3 are for Ge2 post-annealed at 950 °C, and curve 4 is for Ge3 post-annealed at 950 °C. Strong Bragg peak at 26.44° and a weak peak at ~27.4° (shown with arrow) in curve 1 correspond to GeO_2 and Ge(1 1 1) NCs, respectively [9]. Due to the very small size of the NCs in 800 °C annealed sample, Ge related peak is very weak in XRD spectra. After 950 °C annealing, Ge(1 1 1) peak became distinct due to larger size of the NCs as shown in curves 2 and 4. Curve 3 shows both Si(1 1 1) and Ge(3 1 1) peaks after annealing at 950 °C. It is found that the broad Si(1 1 1) peak at 28.4° and Si(3 1 1) peak at 55.9° occur in Ge2 and Ge3 samples only after annealing at 950 °C. The broad Si peaks are the signatures of the formation of Si NCs. Despite the experimental limitations, when Si(1 1 1) or Si(3 1 1) peak width is used to estimate the size of Si NCs using Debye–Scherrer formula, the mean size of the NCs comes out to be ~8 nm. This is similar to the estimated average size of Ge NCs using low frequency Raman spectrum (Table 1 vide infra). Since the average particle size, size distribution and strain in the NCs contribute to the broadening of spectral line shape, actual mean size of Si NCs would be much smaller than the size estimated from Debye–Scherrer formula.

The optical Raman spectrum of Ge1 sample shown in Fig. 2 reveals peaks at 304 cm^{-1} and 435 cm^{-1} corresponding to scattering from optical phonons involving Ge–Ge and Si–Ge stretching motions, respectively [10]. The strong peak at 521.6 cm^{-1} arises from the Si substrate, and weak peaks at ~230 cm^{-1} and ~253 cm^{-1} are signatures of Ge related components. Similar Raman spectrum has been observed by Wu et al. [11] in Ge^+ implanted SiO_2. Single crystalline Ge wafers show a Raman peak at 301.1 cm^{-1}. The observed small upshift of the Raman peak position may be caused by the compressive stress exerted on Ge NCs by the surrounding matrix due to the strong lattice mismatch between Ge and SiO_2 [11].

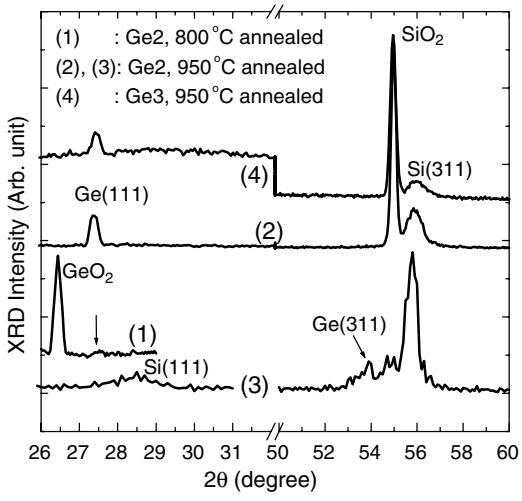

Fig. 1. Grazing incidence X-ray diffraction spectra of Ge implanted and annealed SiO_2/Si layer. Curve 1: annealing at 800 °C for Ge2, and curves 2, 3: annealing at 950 °C for Ge2, curve 4: annealing at 950 °C for Ge3. Curves 1, 2, and 4 are obtained with grazing angle of 2° and curve 3 is obtained with grazing angle of 3°.

Table 1
Ge nanocrystallite mean size estimated from the low frequency Raman scattering data as a function of ion fluence and annealing temperature (T_a)

Ge^+ fluence (cm^{-2})	Ge NC size (nm)	
	$T_a = 800$ °C	$T_a = 950$ °C
3×10^{16}	4.0	6.1
1×10^{17}	5.4	13.0
2×10^{17}	4.1	9.2

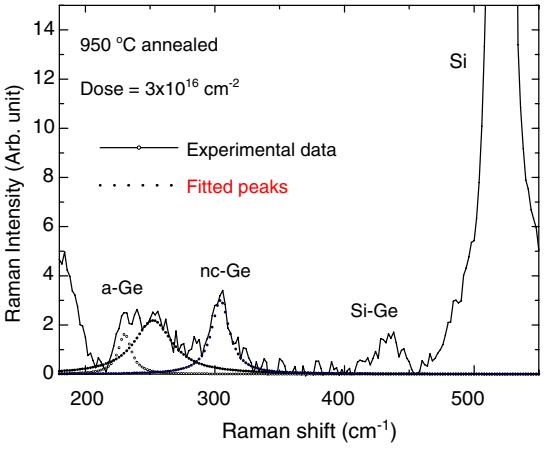

Fig. 2. Optical Raman spectrum of the 950 °C annealed sample implanted with Ge ions. Solid line is the experimental data and the broken lines are fitted Lorentzian line shapes. Bonds responsible for the modes are indicated.

To determine the size of the NCs, low frequency Raman scattering (LFRS) measurements were performed on these samples. LFRS modes arise from the surface acoustic phonons of Ge NCs at the interface between the crystallite and the embedding dielectric matrix, and its frequency is inversely proportional to the size of the NCs [12]. LFRS of 800 °C annealed samples show a peak at 21.2 cm^{-1} in Ge1 and 15.7 cm^{-1} in Ge2 sample. After 950 °C annealing, these peaks shift to 13.8 cm^{-1} and 6.5 cm^{-1}, respectively, indicating the increase in NC size. The average diameter of the NCs estimated from LFRS varies from 4 to 13 nm depending on the ion dose and annealing temperature and shown in Table 1. It is clear from Table 1 that Ge NCs grow in size with the increase of the ion dose and the annealing temperature. It is well known that NCs fabricated by ion implantation show a wide distribution of size

and the measured size is the average of the sizes present in the matrix. In the present study, NCs were biggest at 1×10^{17} ions/cm^2 after 950 °C post-annealing. Details of the LFRS analysis are treated elsewhere [13]. One possible reason for smaller NCs in the highest dose sample (see Table 1) could be related to heavy lattice damage that hinders growth of the NCs during annealing. We found a carbon coating on this sample after implantation, since the implantation was performed for long duration with high beam current. It is likely that this carbon coating may have blocked some of the ions to penetrate the desired depth in the SiO_2 layer, resulting in effectively smaller dose ions than expected. This effective lower dose might have caused the smaller size NCs.

Fig. 3 shows a set of Raman spectra for 950 °C annealed Ge1, Ge2 and Ge3 samples. At low fluence, a sharp peak is observed at 521 cm^{-1} due to Si substrate. At higher fluence ($\geqslant 1 \times 10^{17}$ cm^{-2}), Si peak intensity diminishes and broadens due to ion damage. In addition, another peak emerges at ~503 cm^{-1} in Ge2 sample and becomes prominent at a fluence 2×10^{17} cm^{-2} (Ge3). The inset of Fig. 3 shows the spectra of Ge3 sample and the constituent peaks after subtracting the background. 503 cm^{-1} Raman peak is attributed to Si NCs [14], which are formed as a result of ion impact near the Si/SiO_2 interface. The broad peaks at ~483 cm^{-1} and ~389 cm^{-1} are attributed to amorphous Si and Si–Ge bonds, respectively [10].

During the high-fluence implantation, 300 keV Ge^+ ions reach the SiO_2/Si interface and deposits energy to the surrounding Si atoms. Some of these atoms are segregated in the SiO_2 layer making it a silicon-rich oxide layer. Subsequent heat treatment at 950 °C of the Si supersaturated layer induces the nucleation and growth of the Si NCs near the Si/SiO_2 interface [15]. These Si NCs are detected by XRD and Raman techniques only for high fluence implanted samples. Heat treatment at lower temperature (800 °C) or implantations at low fluence do not induce sufficient segregation of Si atoms and thus Si NC peaks are not detected. Since the phonon confinement, particle size distribution and the strain in the NCs contribute to the line shape broadening of the Raman spectra, mean size of the NCs could not be estimated from the Raman line width. Raman peak at ~503 cm^{-1} corresponds to Si NCs. This is lower by about 18 cm^{-1} than that of bulk Si. If this downshift is due to phonon confinement alone, neglecting the strain effect, the estimated Si NC size would be ~1.4 nm [14]. Although this is an underestimate, the actual Si NC size is expected to be lower than the size of the Ge NCs (as determined from LFRS studies), primarily due to the low density of the Si atoms available for nucleation and growth. It is to be understood that Si NCs grow as a byproduct of the Ge^+ implantation process in SiO_2. This is made possible by choosing the energy of the implanting species such that a large portion of the deposited ion energy is used for mixing at the Si/SiO_2 interface and by subsequent heat treatment to recover the ion-damage and allow growth of the Si NCs [15]. Due to Ge ion implantation, density and size of the Ge NCs are much higher than those of the Si NCs. Time resolved photoluminescence (PL) studies on these samples revealed that the PL decay dynamics in the nanosecond time scale is controlled by the Ge NCs and the defects at the Ge/SiO_2 interface [16]. If the decay dynamics were controlled by the Si nanocrystals, one would have expected a slower decay dynamics.

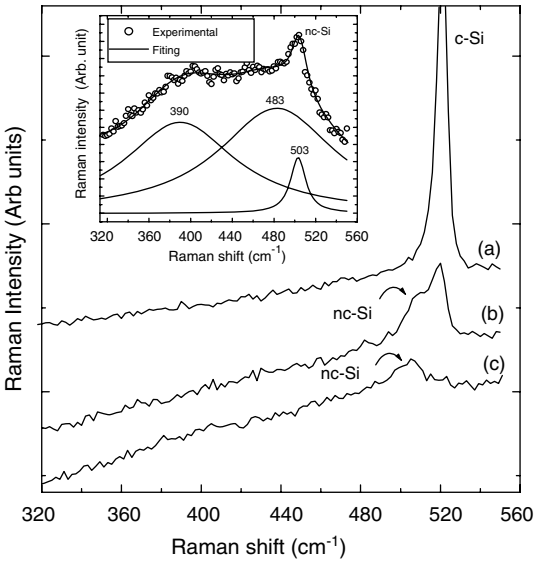

Fig. 3. Optical Raman spectra of the 950 °C annealed samples: (a) Ge1, (b) Ge2 and (c) Ge3. Signature of Si NCs is indicated with arrow for Ge2 and Ge3 samples. The inset shows the background subtracted Ge3 Raman spectrum with constituent peaks fitted to Lorentzian line shapes. Peak positions are denoted by the corresponding wavenumbers.

4. Conclusions

We have synthesized Si NCs in the SiO_2 layer by high fluence Ge ion implantation at room temperature. By choosing an appropriate energy and fluence of the implanted Ge^+ ions and post-implant annealing, Si NCs are formed near the SiO_2/Si interface, in addition to the Ge NCs formed in the SiO_2 matrix. XRD and Raman studies confirm the formation of both Ge NCs and Si NCs in samples implanted with high fluence ($\geqslant 1 \times 10^{17}$ cm^{-2}) and annealed at 950 °C. Si NCs are believed to form as a result of radiation-induced transfer of energy to Si ions and their nucleation and growth under suitable thermodynamic conditions. These results imply that under suitable thermodynamic conditions any energetic ions species could be irradiated at the interface of an immiscible bilayer system to produce nanocrystals of desired species.

Acknowledgements

We are thankful to S. Sarma, A. Srinivasan, P. Magudapathy, S. Dhara, B. Sundaravel, S. Amrithapandian, S. Balaji and David for helps at various stages of this work.

References

[1] R.T. Collins, P.M. Fauchet, M.A. Tischler, Phys. Today 50 (1997) 24.
[2] Y. Cing, T. Jing, C. Hu, IEEE Trans. Elec. Dev. 48 (2001) 696.
[3] M. Nogami, Y. Abe, Appl. Phys. Lett. 65 (1994) 2545.
[4] D.C. Paine, C. Caragianis, T.Y. Kim, Y. Shigesato, T. Ishahara, Appl. Phys. 62 (1993) 2842.
[5] S. Guha, M.D. Pace, D.N. Dunn, I.L. Singer, Appl. Phys. Lett. 70 (1997) 1207.
[6] K.S. Min, K.V. Shcheglov, C.M. Yang, H.A. Atwater, M.L. Brongersma, A. Polman, Appl. Phys. Lett. 68 (1996) 2511.
[7] H. Rong, A. Liu, R. Jones, O. Cohen, D. Hak, R. Nocolascu, A. Fang, M. Paniccia, Nature 433 (2005) 292.
[8] W.K. Choi, W.K. China, C.L. Heng, L.W. Teo, V. Ho, V. Ng, D.A. Antoniadis, E.A. Fitzgerald, Appl. Phys. Lett. 80 (2002) 2014.
[9] S. Guha, M. Wall, L.L. Chase, Nucl. Instr. and Meth. B 147 (1999) 367.
[10] Mi.I. Alonso, K. Winer, Phys. Rev. B 39 (1989) 10056.
[11] X.L. Wu, T. Gao, X.M. Bao, F. Yan, S.S. Jiang, D. Feng, J. Appl. Phys. 82 (1997) 2704.
[12] E. Duval, A. Boukenter, B. Champagnon, Phys. Rev. Lett. 56 (1986) 2052.
[13] P.K. Giri, R. Kesavamoorthy, B.K. Panigrahi, K.G.M. Nair, Solid State Commun. 136 (2005) 36.
[14] R.K. Soni, L.F. Fonseca, O. Resto, M. Buzaianu, S.Z. Weisz, J. Lumin. 83–84 (1999) 187.
[15] V. Ovchinnikov, V. Sokolov, S. Franssila, Microelec. J. 34 (2003) 579.
[16] P.K. Giri, R. Kesavamoorthy, B.K. Panigrahi, K.G.M. Nair, Solid State Commun. 133 (2005) 229.